Progress In Electromagnetics Research, Vol. 146, 143–153, 2014

Transformation inside a Null-Space Region and a DC Magnetic Funnel for Achieving an Enhanced Magnetic Flux with a Large Gradient

Fei Sun[1, 2] and Sailing He[1, 2, *]

Abstract—The idea of transformation inside a null-space region is introduced for the first time, and used to design a novel DC magnetic compressor that concentrates DC magnetic flux greatly and behaves as a DC magnetic funnel. The proposed device can be used as a passive DC magnetic lens to achieve an enhanced DC magnetic field (e.g., 7.9 times or more depending on the size and other parameters of the compressor) with a large gradient (e.g., 450 T/m or more) in free space. After some theoretical approximation, the proposed device can be easily constructed by using a combination of superconductors and ferromagnetic materials. Numerical simulations are given to verify the performance of our device. The proposed method (use a null-space region as the reference space) can be extended to reduce the material requirement when designing other devices with transformation optics.

1. INTRODUCTION

Achieving a higher static magnetic field in a free space region will lead to a revolution in many technical areas, including improving the sensitivity of magnetic sensors [1], improving the resolution of magnetic resonance imaging (MRI) [2], improving the manipulation of drug delivery using magnetic nano-particles [3, 4], etc. Apart from using an active magnet, which requires high power consumption to achieve a high static magnetic field, we can also use passive devices (so-called magnetic lenses) to obtain a high magnetic field without consuming additional energy. Magnetic lenses can cause an external DC magnetic field to converge/focus, and thus give an enhanced DC magnetic field in a specific region.

Traditionally, people simply use superconductors to enhance the background DC magnetic field, which can be used to improve the sensitivity of magnetic sensors [1, 5–8]. However, these devices can only achieve an enhanced DC magnetic field in a very small region of air (e.g., a region with a diameter of 22 mm) with a very low enhancement factor (e.g., about 2 or 3 times). In-depth theoretical guidance on how to design a magnetic lens with desired enhancement by using superconductors is not given in these designs. Future practical applications have greater demand of these passive DC magnetic lenses. For example, we need an enhanced DC magnetic field in a larger free space region with a larger enhancement factor. For some special applications, we may have some additional requirements for these DC magnetic lenses. MRI [2] requires not only the enhancement of the background DC magnetic field in a relatively large free space region, but also needs an enhanced DC magnetic field with high uniformity. For the applications in drug delivery by magnetic nano-particles [3, 4], we need an enhanced DC magnetic field with a high gradient in a distant air region. Traditional magnetic lenses [5–8] cannot achieve these goals. Some novel DC magnetic lenses must be designed for these specific applications and other future potential applications.

Received 17 March 2014, Accepted 7 May 2014, Scheduled 20 May 2014

* Corresponding author: Sailing He (sailing@kth.se).

[1] Centre for Optical and Electromagnetic Research, Zhejiang Provincial Key Laboratory for Sensing Technologies, JORCEP, East Building #5, Zijingang Campus, Zhejiang University, Hangzhou 310058, China. [2] Department of Electromagnetic Engineering, School of Electrical Engineering, Royal Institute of Technology (KTH), Stockholm S-100 44, Sweden.

In recent years, many novel devices for DC magnetic fields have been designed or even verified experimentally, including cloaking for DC magnetic fields [9, 10], DC magnetic concentrators [11–14], DC magnetic lenses [15] and DC magnetic hoses [16] by using a new theory called transformation optics (TO) [17, 18]. These novel DC magnetic devices can perform excellently in some special applications. For example, DC magnetic concentrators based on TO can provide an enhanced DC magnetic field with high uniformity in a large free space region [11–14], which may be used to improve the imaging quality in MRI. Many of these (superconductor-based or mostly TO-based) magnetic lenses are closed structures, which mean they can only provide a good magnetic field enhancement in the free space region inside the lenses. However, in many other important applications, we need an open structure/lens to achieve a high gradient magnetic field in a region (without magnetic materials) far away from the lens.

The high-gradient magnetic field has been widely used in high-gradient magnetic separation (e.g., beneficiation of minerals) [19, 20], micro-fluidic devices [21], biomedicine research (e.g., microchip technology for cell separations [22, 23] and cell manipulations [24], as well as drug delivery by nano-magnetic particles [3, 4]), wastewater treatment technology [25, 26], chemical research (e.g., a high gradient magnetic field that can greatly influence chemical reaction rate [27]), the new generation of materials [28] and so on. Traditionally people obtain a gradient magnetic field simply by using an active magnet, which is an active device and limited by the heat effect. To further develop these technologies and applications (e.g., a more accurate control of drug delivery in a deeper location of a human body), a higher magnetic field with higher gradient is needed. Very recently, we designed an open DC magnetic compressor to achieve an enhanced DC magnetic field with high gradient [15]. Note that this passive compressor can enhance both background DC magnetic field and field gradient. Thus $(\boldsymbol{B}\cdot\nabla)\boldsymbol{B}$ can be amplified, which means the magnetic force will be greatly enhanced passively. This will improve the recent technologies based on gradient magnetic force [19–24]. However, the material requirement of that DC magnetic compressor is very complex (inhomogeneous anisotropic magnetic materials are required), which means it is hard to realize it experimentally. In this paper, we introduce for the first time the idea

Table 1. The main features of various DC magnetic lenses.

DC magnetic lenses	Main features
Traditional magnetic lenses [5–8] using only superconductors	1. An enhanced DC magnetic field in a very small region of air (e.g., a region with a diameter of 22 mm). 2. A very low enhancement factor (e.g., about 2 or 3 times). 3. The enhanced field is inside a closed region.
DC magnetic lenses based on transformation optics in [11–14]	1. Can achieve an enhanced DC magnetic field with high uniformity. 2. The enhancement factor can be very high. 3. The enhanced field is inside a closed region.
DC magnetic hose [16]	Not for enhancing the DC magnetic field but for transferring the DC magnetic field to an arbitrary distance without loss.
DC magnetic compressor [15]	1. Can achieve an enhanced DC magnetic field with high gradient. 2. The enhancement factor can be very high. 3. It is an open structure that can achieve an enhanced field after the back surface of the device. 4. Anisotropic inhomogeneous magnetic materials are needed.
The present DC magnetic compressor	1. Can achieve a higher field gradient with the same size of the one in [15]. 2. Can achieve a higher enhancement with the same size of the one in [15]. 3. It is an open structure that can achieve an enhanced field after the back surface of the device. 4. Only two homogeneous magnetic materials are needed.

of transformation inside a null-space region, and combine this idea with finite embedded transformation (FET) [29] to design a novel open DC magnetic compressor that will have better performance than our previous design [15]. We can get higher enhancement on background field B and higher field gradient and thus higher $(\boldsymbol{B}\cdot\nabla)\boldsymbol{B}$ with the same size of the device. After some theoretical approximations, the proposed compressor can be easily constructed by using the combination of superconductors and ferromagnetic materials, and thus paves a way for future experiment. In order to show the difference of various DC magnetic lenses clearly, we give the main features and limitations of these DC magnetic lenses in Table 1.

2. TRANSFORMATION INSIDE A NULL SPACE REGION

Our design is based on transformation optics [17, 18], which has been widely used to design DC magnetic devices [9–16]. The basic idea is that we can control the DC magnetic field by using magnetic materials with some special permeability. These materials of desired function, called transformed media, are designed by using the coordinate transformation between two spaces: one space is the reference space (a virtual space) and the other is the real space. In this paper, the quantities with or without primes indicate the quantities in the real or the reference space, respectively. For example, we use (x', y', z') and (x, y, z) for the coordinate systems in the real space and the reference space, respectively. The relation between two spaces are established by the coordinate transformation $x' = x'(x, y, z)$, $y' = y'(x, y, z)$ and $z' = z'(x, y, z)$. We can use the following formula to calculate the desired material in the real space [17, 18]:

$$\bar{\bar{\mu}}' = \boldsymbol{A}\bar{\bar{\mu}}\boldsymbol{A}^T/\det(\boldsymbol{A}), \tag{1}$$

where $\boldsymbol{A} = \partial(x', y', z')/\partial(x, y, z)$ is the Jacobian transformation matrix determined by the specific coordinate transformation, and $\bar{\bar{\mu}}$ and $\bar{\bar{\mu}}'$ are relative permeability tensors of the reference space and the real space, respectively. In our previous design [15], the reference space is the free space, which leads to the transformed materials with highly anisotropic inhomogeneous permeability. In the present paper, we use a slab with thickness d filled with some material (called the "null-space" medium) as the reference space. Then we make a space compression FET (similar to our previous transformation in reference [15]) of this null-space slab to obtain a new DC magnetic compressor with a larger enhancement factor than our former design [15]. In the next section, we will show that due to the null-space slab in the reference space, we can make some approximation to greatly reduce the material requirement of our compressor.

The idea of the "null-space" medium has actually been introduced and studied in the case of an electromagnetic wave [30]. Hyperlens, which can surpass the diffraction limit, can be treated as a

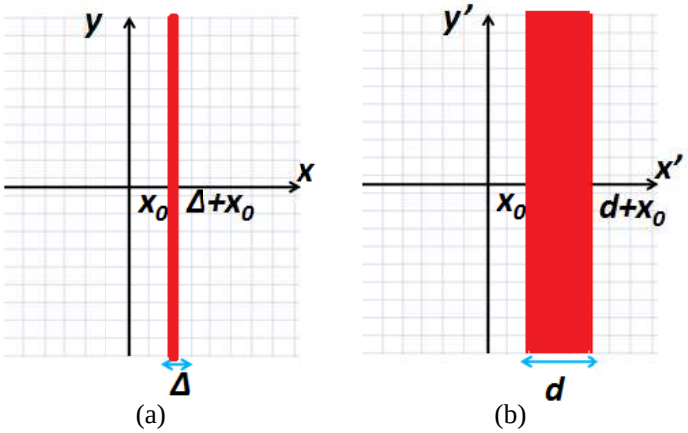

Figure 1. The transformation relation between (a) the reference space and (b) the real space described by Equation (2). A thin slab region $x_0 < x < x_0 + \Delta$ is transformed into a thick slab region $x_0 < x' < x_0 + d$. If Δ approaches zero, we transform a surface (a null-space region) in the reference space into a space region in the real space.

columnar null-space medium [31]. For the present static magnetic field case, the "null-space" medium also plays important roles: the DC magnetic hose, which can transfer the DC magnetic flux to an arbitrary distance without any energy loss (behaving like a special waveguide for DC magnetic field), has been designed recently [16]. This DC magnetic hose is actually a "null-space" medium for the DC magnetic field. Next we briefly review the idea of a "null-space" medium in the DC magnetic field case. As shown in Fig. 1, a very thin slab region $x_0 < x < x_0+\Delta$ in reference space is transformed into a wide slab region $x_0 < x' < x_0+d$ in real space, while keeping other regions identical or giving them translation transformations that do not change the permeability. We can write this linear transformation as follows:

$$x' = \begin{cases} x, & x \le x_0 \\ \dfrac{d}{\Delta}x + \left(1 - \dfrac{d}{\Delta}\right)x_0, & x_0 \le x \le x_0 + \Delta\,; \quad y' = y; \quad z' = z. \\ x - \Delta + d, & x > x_0 + \Delta \end{cases} \tag{2}$$

The corresponding transformation medium can be calculated by [17, 18]:

$$\bar{\bar{\mu}}' = \begin{cases} \text{diag}\left(\dfrac{d}{\Delta}, \dfrac{\Delta}{d}, \dfrac{\Delta}{d}\right) \overset{\text{when}\Delta\to 0}{\to} \text{diag}(\infty, 0, 0), & x_0 \le x' \le x_0 + d \\ 1, & \text{else} \end{cases}. \tag{3}$$

If Δ approaches zero, the slab in the reference space will be reduced to one surface $x = x_0$. In this case, we transform a surface $x = x_0$ in the reference space into a space $x_0 < x' < x_0 + d$ in the real space. Therefore, the space $x_0 < x' < x_0 + d$ in the real space corresponds to a surface (but not a space) in the reference space, which means this space in real space corresponds to a null-space region in the reference space. That is the reason why we use null-space to describe the transformed medium when Δ approaches zero. Many researchers have studied this kind of null-space transformed medium [16, 30]. In this paper, we will use this null-space medium described by Equation (3) as the reference space, and make another transformation inside this null-space medium to design a novel DC magnetic compressor. The reference space now is the medium described by Equation (3), and it can be reduced to a free space or null-space by choosing $\Delta = d$ or 0, respectively. Now we will make the following further compression transformation on this null-space region (see Fig. 2; note that we use null-space medium described by

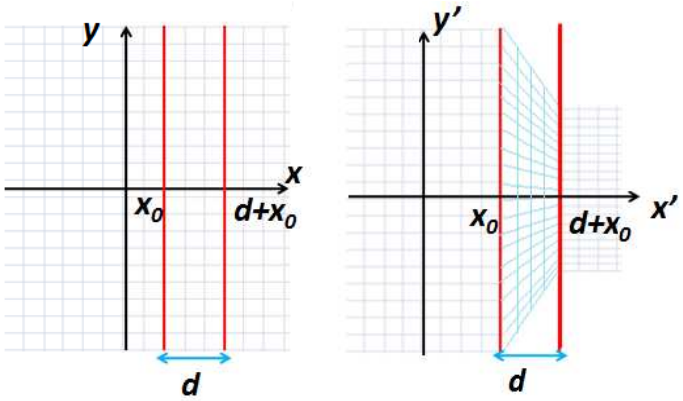

(a) (b)

Figure 2. The transformation relationship between (a) the reference space and (b) the real space described by Equation (4). The medium in the reference space is now described by Equation (3). The slab region $x_0 < x < x_0+d$ (filled with the null-space medium) is compressed in the y direction and the other regions (free space regions) are still undergoing an identical transformation. In the compressed region $x_0 < x < x_0 + d$, the coordinate grid $x = x_c$ (parallel straight lines) is still transformed to $x' = x_c$ and the coordinate grid $y = y_c$ is transformed to $y' = f(x', y_c)$ (compressed lines) whose slope $dy'/dx' = df/dx$ determines the local direction of the transformed grid.

Equation (3) as the reference space in Fig. 2):

$$x' = x$$
$$y' = \begin{cases} y, & x' < x_0 \\ f(x,y), & x_0 \le x' \le x_0 + d \\ y, & x' > x_0 + d \end{cases}, \tag{4}$$
$$z' = z$$

where $f(x, y)$ can be an arbitrary continuous function satisfying $f(x_0, y) = y$ and $f(x_0 + d, y) = My$, which indicates a space compression transformation with $0 < M < 1$. For example we can choose a linear compression function: $f(x, y) = [(M - 1)(x - x_0)/d + 1]y$, which has been used in our previous design [15]. d is the thickness of the device and M determines the compression degree (also the field enhancement degree) of the device. Note that we keep an identical transformation in the regions $x' < x_0$ and $x' > x_0+d$, and therefore they are still free space after the transformation. We only need to calculate

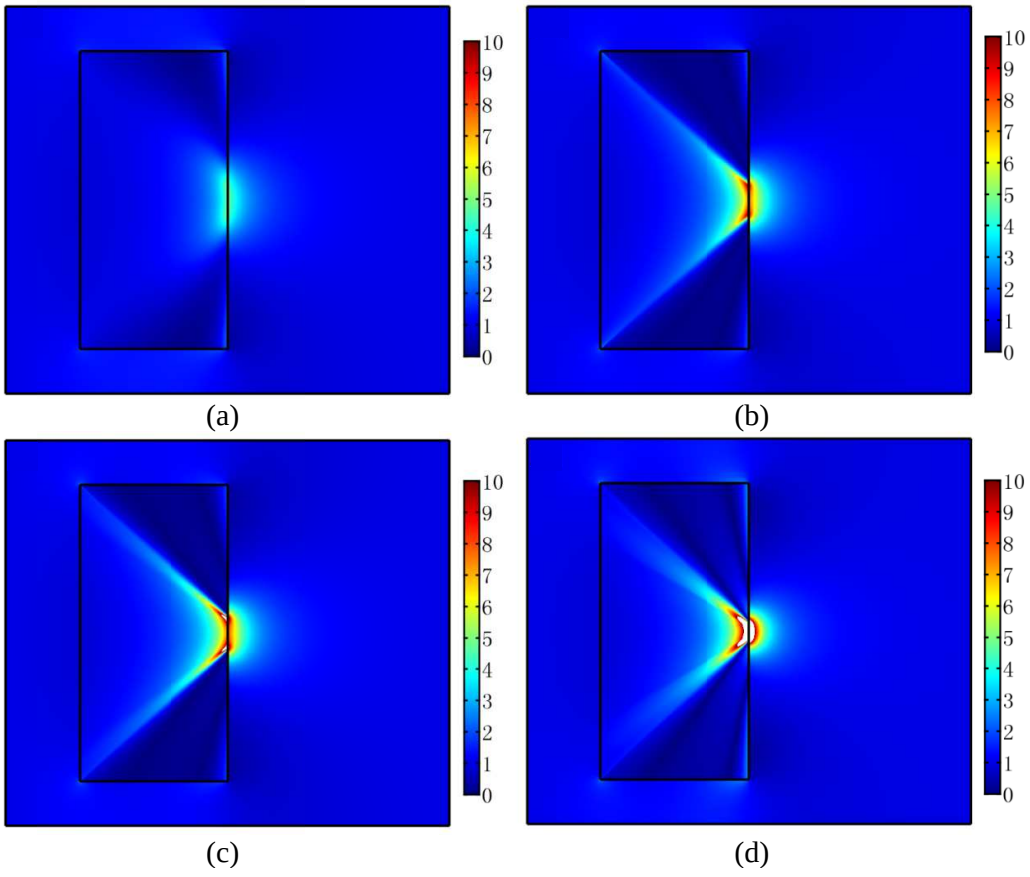

Figure 3. FEM simulation results for the distribution of the total magnetic flux density when a uniformed background static magnetic field $B_b = 1\,\mathrm{T}$ is imposed onto a 2D DC magnetic compressor from left to right. The compressor has height $H = 20\,\mathrm{cm}$ and thickness $d = 10\,\mathrm{cm}$. The transformation function $f(x, y) = [(M - 1)(x - x_0)/d + 1]y$ with $x_0 = 0$ is chosen here. We choose $M = 0.1$ and $\Delta = 10\,\mathrm{cm}$ in (a) $M = 0.1$ and $\Delta = 1\,\mathrm{cm}$ in (b), $M = 0.1$ and $\Delta = 0.1\,\mathrm{cm}$ in (c), and $M = 0.05$ and $\Delta = 0.1\,\mathrm{cm}$ in (d). The maximum enhancement degree in the center region after the compressor is 4.8, 7.6, 7.9 and 15.5 for (a), (b), (c) and (d) respectively. The white regions mean that the magnetic field is larger than the largest value of the color bar.

the transformed medium in the region $x_0 < x' < x_0 + d$, where our compressor is placed:

$$\bar{\bar{\mu}}' = \begin{bmatrix} \frac{d}{\Delta}\Big/\frac{\partial f}{\partial y} & \frac{d}{\Delta}\frac{\partial f}{\partial x}\Big/\frac{\partial f}{\partial y} & 0 \\ \frac{d}{\Delta}\frac{\partial f}{\partial x}\Big/\frac{\partial f}{\partial y} & \left[\left(\frac{\partial f}{\partial x}\right)^2\frac{d}{\Delta} + \left(\frac{\partial f}{\partial y}\right)^2\frac{\Delta}{d}\right]\Big/\frac{\partial f}{\partial y} & 0 \\ 0 & 0 & \frac{\Delta}{d}\Big/\frac{\partial f}{\partial y} \end{bmatrix}. \tag{5}$$

By introducing

$$f_x := \frac{\partial f}{\partial x}; \quad f_y := \frac{\partial f}{\partial y}, \tag{6}$$

for a 2D device, we can rewrite Equation (5) as:

$$\bar{\bar{\mu}}' = \frac{d}{\Delta f_y}\begin{bmatrix} 1 & f_x \\ f_x & \left[(f_x)^2 + (f_y)^2\left(\frac{\Delta}{d}\right)^2\right] \end{bmatrix}. \tag{7}$$

Next we use the finite element method (FEM) to verify the performance of our device. The finite element simulation is conducted by using commercial software COMSOL Multiphysics. For simplicity, we consider a 2D case and choose the following linear compression transformation $f(x, y)$:

$$f(x, y) = \left[\frac{M-1}{d}(x - x_0) + 1\right] y. \tag{8}$$

As shown in Fig. 3, the proposed compressor shows a good compression performance for the DC magnetic field. If Δ decreases from d to zero and the other parameters remain constant, which means that the reference space is changing from a free space to a null-space slab inserted in a free space, the concentration effect increases (compare the results of Figs. 3(a), (b) and (c)). This shows that if we choose a null-space slab inserted in free space, but not a simple free space as the reference space, we can get a more effective field enhancement as well as a higher gradient (see Fig. 4). Note that Fig. 3(a) and Fig. 4(a) to (b) correspond to our previous design in reference [15]. Figs. 3(b) to (d) and Figs. 4(b) to (h) are based on the theory in the null-space medium. The results show that the compressor based on the null-space region in the reference space gives both higher magnification factor and higher field gradient.

The reason for this can be explained using transformation optics. First we explain why the smaller the value of Δ is, the higher the gradient of DC magnetic field can be achieved. From Figs. 1(a) to (b), we can see that if Δ is smaller than d, it means that the coordinate (i.e., the length of each grid) extends along the x (horizontal) direction in the null-space medium (see Equation (2)). Therefore, as Δ decreases from d to zero, the effective length of each grid along the horizontal direction in the null-space medium (described by Equation (3)) increases. In other words, a physical space of thickness d has a length of d along the horizontal direction when filled with air. However, if the space of thickness d is filled with null-space medium, it has an effective length of Δ (smaller). Then we use this null-space medium described by Equation (3) as the reference space in Fig. 2(a). From Figs. 2(a) to (b), we make a compression transformation [along the y (vertical) direction (see Equation (4))] of a slab with thickness d filled by the null-space medium described by Equation (3). A slab with thickness d filled by the null-space medium described by Equation (3) behaves the same as a slab with thickness Δ filled by air. For a fixed physical thickness d, the slab filled with the null-space medium (corresponding to a smaller Δ) in Fig. 2(a) means it has a smaller effective total length along horizontal direction. Therefore for the same compression degree along the vertical direction (i.e., M is the same) from Figs. 2(a) to (b), the null-space medium (corresponding to a smaller Δ) of fixed physical thickness d filled in Fig. 2(a) is equivalent to a smaller total effective thickness Δ along the horizontal direction in the real space, which also means a faster compression inside the device. This leads to the fact that as Δ becomes smaller, we will get an enhanced DC magnetic field with a higher gradient after our compressor as shown in Fig. 4.

Next we will explain why a smaller Δ results in larger field enhancement. Once the compressed DC magnetic field passes through our compressor, it will diverge very quickly in the free space region. The final enhanced DC magnetic field at the output surface of our compressor should be mainly decided by two factors: one is the compression effect of our compressor and the other one is the diverging effect of the free space. When Δ becomes smaller, our compressor can provide a more rapid compression. At the same time, the diverging effect is still the same, as it is still free space after our compressor. Therefore the effect of enhancement will be more obvious (see Figs. 3(a) to (c)). Another thing we should mention is that M $(0 < M < 1)$ also influences the degree of field enhancement: when keeping other parameters unchanged, the smaller the value of M, the higher enhancement (see Figs. 3(c) and (d)). This can also be explained using transformation optics. At the output surface we have $y' = My$, and therefore a smaller M means higher compression (when the other parameters keep the same).

3. REDUCTION METHOD

The performance of our novel DC magnetic compressor has been verified by FEM. Next, we will show that if we choose a null-space slab inserted in free space as the reference space, the required permeability of our compressor can be greatly reduced under some approximations. As the permeability tensor in Equation (7) is symmetrical, we can always diagonalize it [13]. Before we undertake diagonalization, we first make an approximation: considering $\Delta \ll d$ is a very small quantity, and thus $f_x^2 + f_y^2\Delta^2/d^2 \approx f_x^2$,

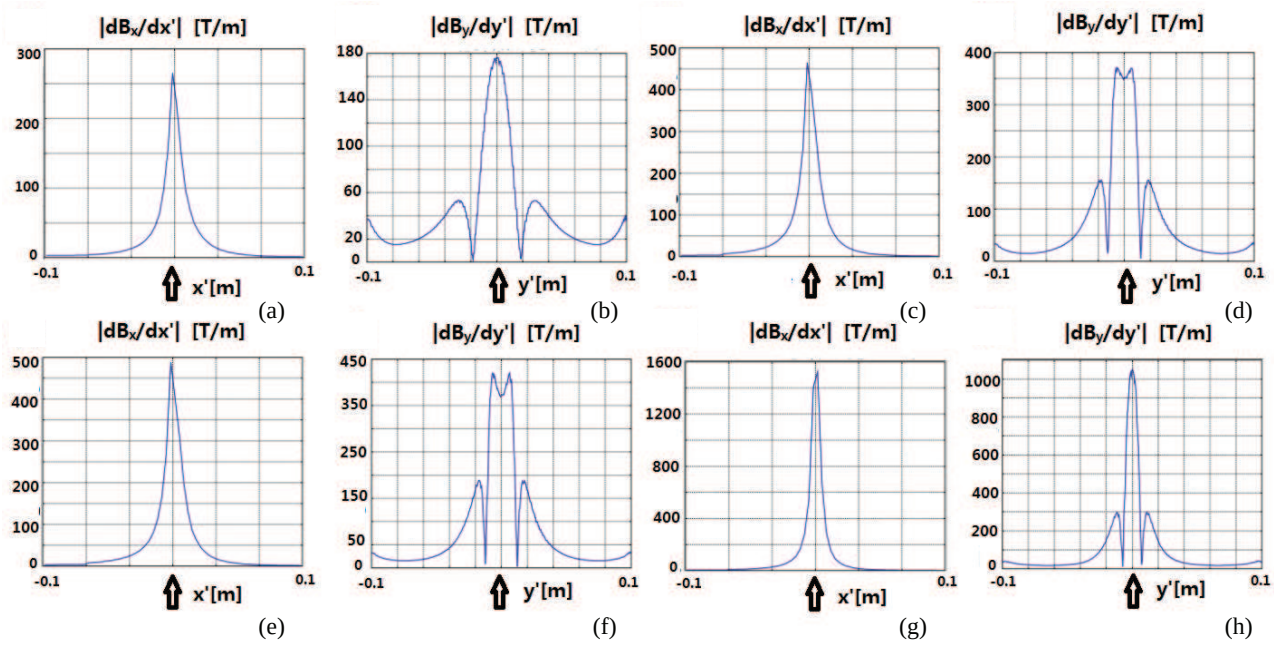

Figure 4. The amplitude of the gradient of the DC magnetic field $\mathrm{d}B_x/\mathrm{d}x$ along the x' direction in the central symmetrical axis of the device: (a), (c), (e), and (g) correspond to the devices in Figs. 3(a), (b), (c), and (d) respectively. The amplitude of the gradient of the DC magnetic field $\mathrm{d}B_y/\mathrm{d}y$ along the y' direction 5 mm after the back surface of the device: (b), (d), (f), and (h) correspond to the devices in Figs. 3(a), (b), (c), and (d) respectively. As Δ decreases, the gradient of the enhanced DC magnetic field increases along both the x' direction and the y' direction. Arrows in (a), (c), (e) and (g) indicate the location of the back surface of the device. Arrows in (b), (d), (f) and (h) indicate the location of the center symmetrical axis of the device. Note that the field gradient is slightly asymmetrical about the arrows in (a), (c), (e), and (g). The reason is that arrows in (a), (c), (e), and (g) indicate the location of the back surface of the device, which is the boundary of two different materials: before these arrows (i.e., $-0.1\,\mathrm{m} < x' < 0$), it is filled with magnetic materials (our magnetic compressor); after these arrows (i.e., $0 < x' < 0.1\,\mathrm{m}$), it is free space.

the permeability of our compressor can therefore be approximately described by:

$$\bar{\bar{\mu}}' \approx \frac{d}{\Delta f_y}\begin{bmatrix} 1 & f_x \\ f_x & f_x^2 \end{bmatrix}. \tag{9}$$

Then this symmetrical tensor can be easily diagonalized to the following form:

$$\bar{\bar{\mu}}' \approx \frac{d}{\Delta f_y}\begin{bmatrix} 1 & f_x \\ f_x & f_x^2 \end{bmatrix} \overset{\text{coordinate system rotation}}{\rightarrow} \text{diag}\left(\frac{d}{\Delta}\frac{1}{f_y}\left(1+f_x^2\right), 0\right) \overset{\Delta\rightarrow 0}{\rightarrow} \text{diag}(\infty, 0). \tag{10}$$

Equation (10) shows that we can realize this anisotropic medium by using some layered ideal superconductors ($\mu = 0$) and ideal ferromagnetic materials ($\mu = \infty$) [13]. The orientation of this multilayer is the principal axis angle (the rotation angle between the x'-y' system and the local coordinate system), which can be given as [13]:

$$\tan(2\theta) = \left(\frac{2\mu'_{xy}}{\mu'_{xx} - \mu'_{yy}}\right) = \frac{2f_x}{1 - f_x^2}. \tag{11}$$

With the relation of $\tan(2\theta) = 2\tan\theta/(1 - \tan^2\theta)$, Equation (11) gives:

$$\tan\theta = f_x = \frac{\partial f(x,y)}{\partial x} = \frac{\partial y'}{\partial x'}. \tag{12}$$

Therefore θ corresponds to the slope of the transformation function $f(x, y)$. We should note that the shape of function $f(x, y)$ can be arbitrary provided that it is a continuous function and satisfies $f(x_0, y) = y$ and $f(x_0 + d, y) = My$. Therefore the slope of this function (also θ) can also be chosen arbitrarily provided that it changes continuously.

Now we obtain two important results (Equations (10) and (12)) which can greatly reduce the materials' requirement of our compressor: provided that Δ approaches zero, we can simply utilize

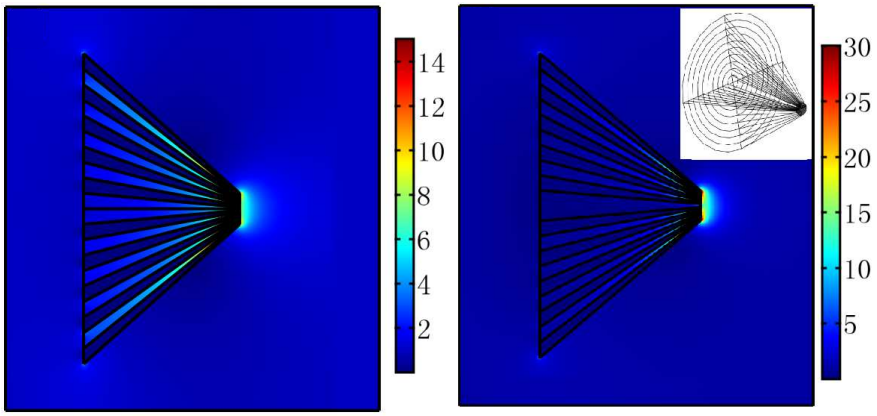

Figure 5. FEM simulation results for the distribution of the total magnetic flux density when a uniformed background static magnetic field $B_b = 1\,\text{T}$ is imposed onto the reduced compressor from left to right. (a) The 2D reduced compressor is composed by 10 superconductor layers with relative permeability $\mu = 10^{-6}$ and 10 ferromagnetic material layers with relative permeability $\mu = 10^6$. The height and thickness of the reduced compressor are the same as the structures in Fig. 3: height $H = 20\,\text{cm}$ and thickness $d = 10\,\text{cm}$. The transformation function $f(x, y)$ is $f(x, y) = [(M-1)(x-x_0)/d+1]y$ with $M = 0.1$ and $x_0 = 0$. (b) A 3D DC magnetic compressor generated through the rotation of the 2D one in (a) along the x'-axis. The insert in (b) shows the 3D geometrical shape of this funnel compressor. The maximum degree of enhancement in the center region after the back surface of the compressor is about 9 and 14.1 times in (a) and (b) respectively. Note that (a) is a 2D FEM simulation of a 2D flat structure; magnetic field is in the plane. (b) Is a 3D FEM simulation of a 3D funnel structure (rotation symmetric on x' axis); we only plot a cross section of the whole structure. The cross section of the 3D funnel structure has the same shape as the 2D flat structure.

two magnetic materials with relative permeabilities $\mu_1 = 0$ (ideal superconductor) and $\mu_2 = \infty$ (ideal ferromagnetic material) layer by layer to realize our compressor approximately. The boundaries of these multilayered materials Γ (whose slopes stand for the local principle angle θ) can be arbitrarily chosen provided that it changes continuously and satisfies the condition of compression transformation: assuming that the intersection between the input surface of the compressor and Γ is $(x_0,\, y_A)$ and the intersection with the output surface of the compressor and Γ is $(x_0 + d,\, y_B)$. Thus $y_B = My_A$ (with $0 < M < 1$) should be satisfied.

This feature can also be understood in another way: as the reference space is a null-space slab when $\Delta \to 0$, we can approximately realize it by using an ideal superconductor and ferromagnetic material, layer by layer. In addition, the orientation of this multilayer is parallel to the x'-axis. If we apply the space compression transformation Equation (4) directly onto this multilayer structure, we can also obtain the desired compressor. Considering that the permeabilities of the ideal superconductor and ferromagnetic material are zero and infinitely large, respectively, the compression transformation does not change the material but only changes their shapes. This means that the ideal superconductor and ferromagnetic material will still be an ideal superconductor and ferromagnetic material respectively, but their shapes will be changed according to the specific transformation function $f(x,\, y)$. This is similar to the case that the perfect electric conductor (PEC) will still be a PEC after the transformation, but different shapes in electromagnetic wave cases [32].

Next we use FEM to verify this reduction method of our compressor. We choose 10 superconductor layers and 10 ferromagnetic material layers to build a reduced compressor of the same geometrical size as the structures used in Fig. 3 (thickness $d = 0.1\,\mathrm{m}$, height $H = 0.2\,\mathrm{m}$). We choose the simplest curves (straight lines) as boundaries Γ and obtain a maximum enhanced degree of about 9 times in the center region after our reduced compressor (see Fig. 5(a)). We can simply extend our compressor from 2D to 3D by rotating the 2D one along its symmetrical axis. Then we will obtain a 3D funnel structure (see Fig. 5(b)). We use FEM simulation to verify the performance of this 3D DC magnetic funnel. In this case we obtain about a maximum 14.1-time-enhancement in the center region after the back surface of our 3D DC magnetic funnel.

4. SUMMARY AND DISCUSSION

Further transformation inside a null-space region has been explored in this paper. The present idea of further transformation inside a null-space region can be extended to reduce the material requirement of other devices based on transformation optics (especially for simplifying some complex inhomogeneous medium).

A novel DC magnetic compressor, which can achieve a DC magnetic field enhancement with a high gradient, has been designed by using compression transformation inside a null-space slab. Compared with previous designs based on compression transformation inside a free space slab region [15], the proposed compressor has the following advantages: 1) it can passively achieve a higher degree of field enhancement. Fig. 3 shows that the maximal enhancement degree gradually increases from 4.8 to 7.9 as the reference space changes gradually from a free space region to a null-space region. 2) It can passively achieve a higher gradient of the field. As shown in Fig. 4, the maximal gradient of the field increases from about $260\,\mathrm{T/m}$ to $490\,\mathrm{T/m}$ along x' direction and from about $175\,\mathrm{T/m}$ to $425\,\mathrm{T/m}$ along y' direction when the reference space changes gradually from a free space region to a null-space region. 3) The requirement of the materials' permeability is much simper. As shown in Equation (10), we can simply use superconductors and ferromagnetic materials to realize this compressor just as has been done for other DC magnetic devices [11, 16].

The function of this novel DC magnetic compressor is like a funnel that concentrates DC magnetic flux. Compared with other DC magnetic compressors designed by TO [11–14], our compressor has two important features. Firstly, the proposed compressor is an open structure that can achieve an enhanced gradient DC magnetic field after the back surface of the device, which can be used for some special applications (e.g., drug delivery via magnetic particles). Secondly, after some approximation, the material requirement of the proposed compressor is found to be very simple, which can be approximately constructed by using a combination of superconductor and ferromagnetic materials.

Note that the magnetic force is proportional to $(\boldsymbol{B} \cdot \nabla)\boldsymbol{B}$, and our DC magnetic compressor can

both amplify the background DC field B and produce a high gradient passively. It means that we can greatly enhance the magnetic force passively by using our DC magnetic compressor. Our study will lead a new way to the development of DC magnetic field enhancement by passive devices and provide many potential practical applications in the future (e.g., drug delivery by magnetic nano-particles in deeper tissues, DC magnetic field focusing, high magnetic force generation, cell manipulations by gradient magnetic field, high-gradient magnetic separation, etc.).

ACKNOWLEDGMENT

This work is partially supported by the National High Technology Research and Development Program (863 Program) of China (No. 2012AA030402), the National Natural Science Foundation of China (Nos. 61178062 and 60990322), the Program of Zhejiang Leading Team of Science and Technology Innovation, Swedish VR grant (# 621-2011-4620) and SOARD. Fei Sun thanks the China Scholarship Council (CSC) No. 201206320083.

REFERENCES

1. Ripka, P. and M. Janosek, "Advances in magnetic field sensors," *IEEE Sens. J.*, Vol. 10, 1108–1116, 2010.
2. Brown, M. A. and R. C. Semelka, *MRI: Basic Principles and Applications*, Wiley-Blackwell, 2010.
3. Veiseh, O., J. W. Gunn, and M. Zhang, "Design and fabrication of magnetic nanoparticles for targeted drug delivery and imaging," *Advanced Drug Delivery Reviews*, Vol. 62, No. 3, 284–304, 2010.
4. Dobson, J., "Magnetic micro- and nano-particle-based targeting for drug and gene delivery," *Nanomedicine*, Vol. 1, No. 1, 31–37, 2006.
5. Matsumoto, S., T. Asano, T. Kiyoshi, and H. Wada, "Magnetic flux concentration using YBCO hollow and solid cylinders," *IEEE Trans. Appl. Supercond.*, Vol. 14, 1666–1669, 2004.
6. Zhang, Z. Y., S. Choi, S. Matsumoto, R. Teranishi, G. Giunchi, A. F. Albisetti, and T. Kiyoshi, "Magnetic lenses using different MgB2 bulk superconductors," *Supercond. Sci. Technol.*, Vol. 25, No. 2, 025009, 2012.
7. Asano, T., K. Itoh, S. Matsumoto, T. Kiyoshi, H. Wada, and G. Kido, "Enhanced concentration of the magnetic flux in a superconducting cylinder," *IEEE Trans. Appl. Supercond.*, Vol. 15, No. 2, 3157–3160, 2005.
8. Kiyoshi, T., S. Choi, S. Matsumoto, T. Asano, and D. Uglietti, "Magnetic flux concentrator using Gd-Ba-Cu-O bulk superconductors," *IEEE Trans. Appl. Supercond.*, Vol. 19, No. 3, 2174–2177, 2009.
9. Gomory, F., M. Solovyov, J. Souc, C. Navau, J. Prat-Camps, and A. Sanchez, "Experimental realization of a magnetic cloak," *Science*, Vol. 335, No. 6075, 1466–1468, 2012.
10. Supradeep, N. and Y. Sato, "DC magnetic cloak," *Advanced Materials*, Vol. 24, No. 1, 71–74, 2012.
11. Navau, C., J. Prat-Camps, and A. Sanchez, "Magnetic energy harvesting and concentration at a distance by transformation optics," *Phys. Rev. Lett.*, Vol. 109, 263903, 2012.
12. Sun, F. and S. He, "Create a uniform static magnetic field over 50 T in a large free space region," *Progress In Electromagnetics Research*, Vol. 137, 149–157, 2013.
13. Sun, F. and S. He, "DC magnetic concentrator and omnidirectional cascaded cloak by using only one or two homogeneous anisotropic materials of positive permeability," *Progress In Electromagnetics Research*, Vol. 142, 683–699, 2013.
14. Sun, F. and S. He, "Novel magnetic lens for static magnetic field enhancement," *PIERS Proceedings*, 1689–1691, Stockholm, Sweden, Aug. 12–15, 2013.
15. Sun, F. and S. He, "Static magnetic field concentration and enhancement using magnetic materials with positive permeability," *Progress In Electromagnetic Research*, Vol. 142, 579–590, 2013.
16. Navau, C., J. Prat-Camps, O. Romero-Isart, J. I. Cirac, and A. Sanchez, "Magnetic hose: Routing and long-distance transportation of magnetic fields," arXiv: 1304.6300, 2013.

17. Leonhardt, U. and T. G. Philbin, *Geometry and Light: Science of Invisibility*, Dover, 2010.
18. Pendry, J. B., D. Schurig, and D. R. Smith, "Controlling electromagnetic fields," *Science*, Vol. 312, No. 5781, 1780–1782, 2006.
19. Kolm, H. H., "The large-scale manipulation of small particles," *IEEE Transactions on Magnetics*, Vol. 11, No. 5, 1567–1569, 1975.
20. Svoboda, J., *Magnetic Techniques for the Treatment of Materials*, 641, Kluwer Academic Publishers, Dordrecht, 2004.
21. Choi, J.-W., T. M. Liakopoulos, and C. H. Ahn, "An on-chip magnetic bead separator using spiral electromgnets with semi-encapsulated permalloy," *Biosensors and Bioelectronics*, Vol. 16, No. 4, 409–416, 2001.
22. Yavuz, C. T., A. Prakash, J. T. Mayo, and V. L. Colvin, "Magnetic separations: From steel plants to biotechnology," *Chemical Engineering Science*, Vol. 64, No. 10, 2510–2521, 2009.
23. Inglis, D. W., R. Riehn, J. C. Sturm, and R. H. Austin, "Microfluidic high gradient magnetic cell separation," *Journal of Applied Physics*, Vol. 99, No. 8, 08K101, 2006.
24. Yeunf, S. W. and I. M. Hsing, "Manipulation and extraction of genomic DNA from cell lysate by functionalized magnetic particles for lab on a chip applications," *Biosnensors and Bioelectronics*, Vol. 21, No. 7, 989–997, 2005.
25. Coey, J. M. D. and S. Cass, "Magnetic water treatment," *Journal of Magnetism and Magnetic Materials*, Vol. 209, No. 1, 71–74, 2000.
26. Karapinar, N., "Magnetic separation of ferrihydrite from wastewater by magnetic seeding and high-gradient magnetic separation," *International Journal of Mineral Processing*, Vol. 71, No. 1, 45–54, 2003.
27. Aoyagi, S., A. Yano, Y. Yanagida, E. Tanihira, A. Tagawa, and M. Iimoto, "Control of chemical reaction involving dissolved oxygen using magnetic field gradient," *Chemical Physics*, Vol. 331, No. 1, 137–141, 2006.
28. Jin, F., Z. Ren, W. Ren, K. Deng, Y. Zhong, and J. Yu, "Effects of a high-gradient magnetic field on the migratory behavior of primary crystal silicon in hypereutectic Al-Si alloy," *Science and Technology of Advanced Materials*, Vol. 9, No. 2, 024202, 2008.
29. Rahm, M., S. A. Cummer, D. Schurig, J. B. Pendry, and D. R. Smith, "Optical design of reflectionless complex media by finite embedded coordinate transformations," *Phys. Rev. Lett.*, Vol. 100, 063903, 2008.
30. He, Q., S. Xiao, X. Li, and L. Zhou, "Optic-null medium: Realization and applications," *Opt. Express*, Vol. 21, No. 23, 28948–28959, 2013.
31. Wang, W., L. Lin, X. Yang, J. Cui, C. Du, and X. Luo, "Design of oblate cylindrical perfect lens using coordinate transformation," *Opt. Express*, Vol. 16, No. 11, 8094–8105, 2008.
32. Chen, H., X. Zhang, X. Luo, H. Ma, and C. T. Chan, "Reshaping the perfect electrical conductor cylinder arbitrarily," *New Journal of Physics*, Vol. 10, 113016, 2008.